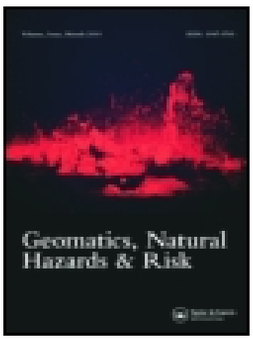

Geomatics, Natural Hazards and Risk

ISSN: 1947-5705 (Print) 1947-5713 (Online) Journal homepage: http://www.tandfonline.com/loi/tgnh20

The impacts of 2008 snowstorm in China on the ecological environments in the Northern South China Sea

Dongyang Fu, Danling Tang & Gad Levy

To cite this article: Dongyang Fu, Danling Tang & Gad Levy (2017): The impacts of 2008 snowstorm in China on the ecological environments in the Northern South China Sea, Geomatics, Natural Hazards and Risk

To link to this article: http://dx.doi.org/10.1080/19475705.2017.1292559

Published online: 28 Feb 2017.

GEOMATICS, NATURAL HAZARDS AND RISK, 2017
http://dx.doi.org/10.1080/19475705.2017.1292559

Taylor & Francis
Taylor & Francis Group

The impacts of 2008 snowstorm in China on the ecological environments in the Northern South China Sea

Dongyang Fu[a], Danling Tang[b,d] and Gad Levy[b,c]

[a]Lab of remote sensing & information technology, Guangdong Ocean University, Zhanjiang, China; [b]State Key Laboratory of Tropical Oceanography, South China Sea Institute of Oceanology, Chinese Academy of Sciences, Guangzhou, China; [c]Danling Tang, South China Sea Institute of Oceanology, Chinese Academy of Sciences, 164 West XinGang Road, Guangzhou, China, 510301; [d]Gad Levy, west Research Associates, Inc. 4118 148th Ave NE,Redmond, WA 98052-5164, USA

ABSTRACT

At the beginning of 2008, disastrous weather with snowstorms truck South China. Analysis of satellite and in situ data revealed obvious changes in ecological environments in the northern South China Sea after snowstorms. The sea surface temperature (SST) data from NOAA and Moderate Resolution Imaging Spectroradiometer (MODIS) from 2000 to 2013, and the chlorophyll-a (Chla) concentration from MODIS are analysed. In the study area, the multiple-day-averaged SST dropped by 20.01% and Chla concentration increased by 22.42% during and after snowstorm. SST decreased more significantly and Chla increased in the coastal waters, while suspended sediment concentration (SSC) increased more remarkably offshore. The biggest drop of SST reached 6°C and striking elevation in Chla with 52.55% in the Taiwan Strait, and SSC changed significantly near to the Taiwan bank after the snowstorm. Further analysis indicated that the remarkable reductions in SST were caused by large cold water input from Min-Zhe coastal water and the Pearl River Estuary, as a result of strong sea-land-air interaction in the coastal waters during the snowstorm. The increase in Chla may be related to the abundant nutrients from the plenty of cold water, a strong front and vertical mixing in the coastal waters.

ARTICLE HISTORY
Received 5 January 2016
Accepted 4 February 2017

KEYWORDS
Snowstorm; Northern South China Sea (NSCS); SST; chlorophyll-a concentration; suspended sediment concentration(SSC); coastal waters; offshore waters; temperature front

1. Introduction

The South China Sea (SCS) is the largest marginal sea of the Western Pacific. Generally, the northern area of it ranges from the west of the Luzon Strait (LZS), southwest of Taiwan Island (TWI), to the north of 18 °N of SCS, which is in the south of the East China sea (ECS). From October to March in the following year, this area is controlled by the winter northwest monsoon with average wind speed about 8–11 m/s , meanwhile the precipitations mainly happen in midsummer, effected by monsoon and tropical hurricane, with the amount of the annual rainfall about 1100–1800 mm (Yan et al. 1993). In the Northern South China Sea (NSCS), the thickness of the mixed layer is usually only 30–50 m; however, it can reach to 75 m in winter while the sea surface temperature (SST) of the coastal waters is about 21 °C (Wang et al. 2002). The NSCS has complex circulation and hydrodynamic environment because it is affected by the strong Kuroshio with high temperature and salinity and intrusions of currents from Taiwan Strait (TWS), Fujian-Zhejian (Min-Zhe) coastal

CONTACT Danling Tang lingzistdl@126.com

waters (MZCW) coming from Yangtze River (YR) and discharge from the Pearl River (PR), as well as alternating monsoons (Liu et al. 2003; Fu et al. 2014, 2016).

A severe weather event with wide-range sustained low-temperature, freezing rain and sleet took place in Southern China from 11th January to 2nd February 2008. This disaster was extremely severe in terms of its spatial extent, duration and damage, affecting Shanghai (SH), Zhejiang (Zhe), Fujian (Min), Anhui (Wan), Guangdong (Yue), Henan (Yu), Jiangxi (Gan), Jiangshu (Shu), Hunan (Xiang), Guizhou (Qian) and Guangxi (Gui), among other areas, and causing substantial mortality of wild fish and 80% loss of caged Mariculture fish (Chang et al. 2009, 2013). The damaged area of the fishery industry in Guangdong province exceeded 0.17 million hectares and the economic losses to the fishery industry were as high as 6 billion Yuan. At the same time, the disaster caused enormous damage to the environment and greatly influenced people's life.

Some scholars thought that the sea temperature of middle-east Pacific Ocean of the equator entered into La Nina status with booming development from August 2007 to January 2008. This strong La Nina event impacted the NSCS and it was one of important reasons that affected the wide-range sustaining low-temperature, freezing rain and sleet disastrous weather in the Southeast of China (Zheng et al. 2008; Gao et al. 2008). The convergence in Southeast China of the cold air from Eurasia and warm/moist air from the Indian Ocean and SCS caused conditions of freezing rain and sleet in early 2008 in Southeast China (Ma 2009; Shi et al. 2010) (A in Figure 1(a)). During this event, much MZCW from the Yangtze River Estuary (YRE) and the discharge form Pearl River Estuary (PRE) was injected into the TWS and NSCS, bringing a great deal of sand and nutrients. The sea–land–air interaction was enhanced with larger-than-normal discharge and colder temperatures (B in Figure 1(a)) (Shang et al. 2012; Liao et al. 2013; Wang et al. 2013). At the same time, the Kuroshio stream entered the NSCS via LZS (Lan et al. 2009; Shang et al. 2012; Liao et al. 2013; Vigan et al. 2014), and its warm seawater interaction with the cold diluted water impacted the ecological environment (C in Figure 1(a)).

Sea surface temperature (SST) is a comprehensive indicator of the interaction of marine thermodynamic processes. It is not only an important physical parameter for studying humidity and heat exchange across the sea–land–air interface, but also the most intuitive variable for marine studies (Chu et al. 1997; Bao et al. 2002). Chlorophyll-a (Chla) concentration, an index of phytoplankton biomass, is another important indicator of changing conditions in marine ecosystems and climate (Tang et al. 1998, 2002, 2004b, 2004a; Babin et al. 2004). Likewise, the suspended sediment concentration (SSC) in the sea is an important water quality parameter that can directly influence optical properties, such as water transparency, turbidity, water colour, etc. (*Tassan, S.*, 2003; Yan and Tang 2009), and its absorption coefficient has significant influences on ocean biogeochemical processes (Sipelgas et al. 2006; Liu et al. 2010, 2012).

In order to understand the impacts of the 2008 snowstorm on ocean ecosystem, especially in the NSCS, it is important to study the spatial and temporal distribution of SST, Chla and SSC in the area influenced by the event, as well as the mechanism of these changes, as done in this paper.

2. Study area, data and methods

2.1. Study area

The study area is the NSCS and TWS, from 110°E to 122°E, and 19°N to 27°N (blue box in Figure 1 (a)). It receives a large volume of freshwater discharge from the PRE and the YRE (Shang et al. 2012; Liao et al. 2013), is controlled by northeast monsoon in winter (Lan et al. 2009; Vigan et al. 2014) and is invaded by the Kuroshio through the LZS (Shaw & Chao 1994; Shang et al. 2012; Liao et al. 2013). To analyse the impacts of the snowstorm on the ocean environment, we divide the study area into 16 bins of 2°×2°, with Bins 1–9 (shaded portion in Figure 1(b)) for coastal waters (Fujian, Guangdong and the TWS) and Bins 10–16 for offshore waters far away from landmass.

2.2. In situ data

We obtained climatological monthly mean temperature data of Guangdong province in winter (December to February.) for the period of 2007–2013, by averaging temperature of the same month at 86 national meteorological stations in the province. The monthly mean discharge and the surface water temperature data in February from 2006 to 2012 was obtained from Tianhe and Wanshan Stations (the red and blue dots in Figure 1(b)) near the PRE, and in January and February from 2006 to 2012 from Datong Station (blue triangle in Figure 1(a)) near the YRE, respectively.

2.3. Remote sensing data

We analysed daily level-3 SST data with 1.1 km resolution obtained from the AVHRR sensor on the National Oceanic and Atmospheric Administration (NOAA) satellites (12–18 series) and Aqua/Terra Moderate Resolution Imaging Spectroradiometer (MODIS) from 2000 to 2013; and Chla data (2000–2009) and SSC data from Aqua/Terra MODIS before and after the snowstorm. All data-sets with a resolution of about 1.1 km were archived at and supplied by the State Key Laboratory of Satellite Ocean Environment Dynamics (Second Institute of Oceanography, State Oceanic Administration (SIO/SOA), Hangzhou, China). Surface wind data with a spatial resolution of $0.25^\circ \times 0.25^\circ$ and 24 h time interval was obtained from the National Climatic Data Center (NCDC) reanalysis archived by the NOAA(http://www.ncdc.noaa.gov /). In this study, 'before snowstorm' refers to the 17 days period (25th December 2007– 10th,January 2008); 'during and after snowstorm' refers to the following 41 days (from 11th January to 20th February, 2008. Because both the duration of the sleet and snowmelt time were about 20 days, respectively, and most of the remote sensing data were lost due to the extended period of bad weather, therefore, 41 days was taken as the effect time by snowstorm).

2.4. Methods

The SSC and Chla were retrieved from the Aqua/MODIS and Terra/MODIS data using the SeaWiFS Data Analysis System (SeaDAS, He et al. 2014). The data fusion of remote sensing data for multi-day averages (MDA) was done using the algorithm by Fu et al. (2009), and the processing of Chla and SSC data was carried out through a log10 transformation. As the duration of freezing rain and snowstorm weather conditions was very long, much of the remote sensing data of SST, Chla and SSC were missing due to low/no visibility, so the MDA-Chla and SSC before the snowstorm in each bin were calculated as where covered by valid data of remote sensing as that of during and after snowstorm.

3. Results

3.1. SST and air temperature drops during and after the snowstorm

The SST in the NSCS decreased significantly during and after the snowstorm in early 2008, especially in the coastal waters (Figure 2(a, b and f)). The MDA-SST in the study area was 21.73 °C before the snowstorm, but only 17.73 °C during and after the snowstorm, reflecting an average drop of 4 °C, and a remarkable temperature front aligned in the southwest–northeast direction formed through TWS (Figure 2(b)). The SST in the coastal waters (Bins 1–9) decreased by 5.34 °C, while that in offshore areas (Bins 10–16) dropped by only 2.26 °C (Figure 2(f)). What is more remarkable, the average change of SST in Bins 1, 2, 3 and 4 reached 5.99 °C, showing as a 'dark-blue water trough' in the TWS. In addition, Bins 6, 7 and 8 near the PRE had the second largest drop with an average temperature drop of 4.95 °C. Due to the cloudy weather conditions, which resulted in partial data loss (the blank areas in Figure 2), and the interpolation by the software used for drawing in areas such as 10 and 11, the SST in this area shows as relatively low (dark blue). The bins with the

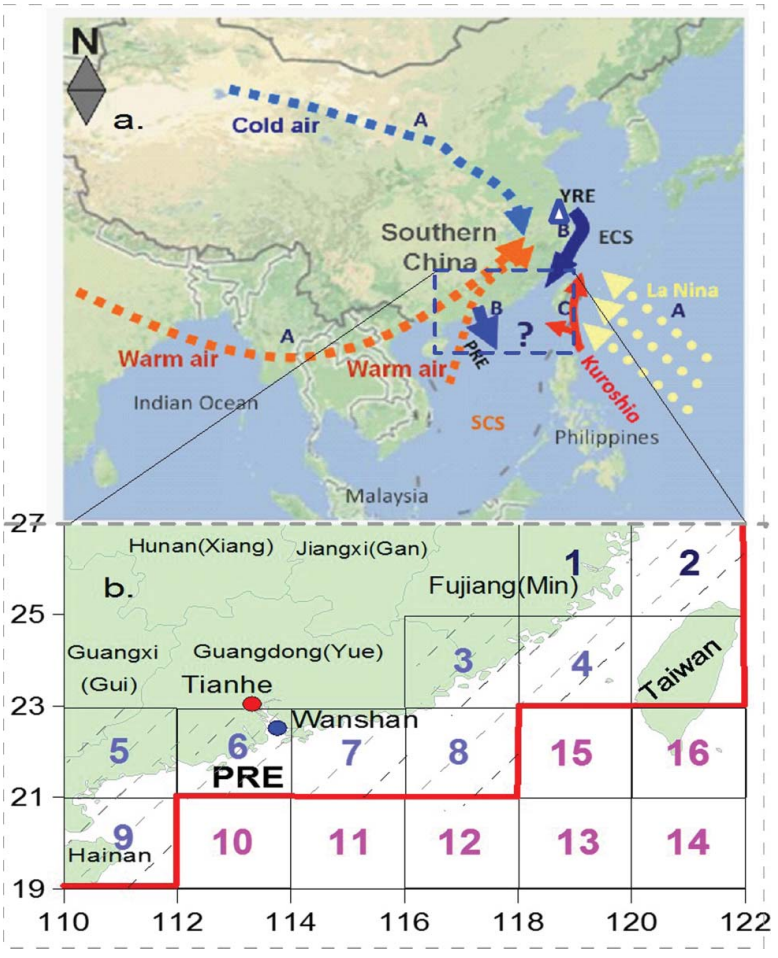

Figure 1. (a) A schematic depiction of the ocean–land–air interaction before and after the snowstorm in South China, NSCS and Taiwan Strait in early 2008. Dashed arrows (A): air flow (light blue: cold air; light red: warm air; light yellow: La Nina flow); solid arrows (B and C): ocean currents (dark blue: diluted water from the YRE; blue: diluted water from the PRE; red arrow: Kuroshio); (b) The study area, divided into16 bins of $2^{\circ} \times 2^{\circ}$. Bins 1–9 are the coastal waters (north and west of the red line), and Bins 10–16 are the offshore area (south and east of the red line). The red and blue dot in the PRE and the blue triangle in the YRE area mark the locations of Tianhe, Wanshan and Datong hydrometric stations, respectively. To view this figure in colour, please see the online version of the journal.

smallest SST reduction were Bins 13 and 14 around the LZS, dropping by 1.17 °C and 0.48 °C, respectively.

Three MODIS images on 5th January, 21th January and 15th February with the lowest SST data loss are selected (Figure 2(c, d and e)), being the best images with the largest one-day areal coverage of the study area before, during and after the snowstorm. SST values in excess of 24 °C in part of the NSCS on 5th January covered a larger area than that on 21th January and on 15th February, and the highest SST values before and after the snowstorm were observed in the LZS. Moreover, there were well-marked cold tongues (dark-blue colour) from the YRE along the Min-Zhe coast, stretching to the PRE of Guangdong province. Both during (Figure 2(d)) and after (Figure 2(e)) the snowstorm, there was a remarkable drop in SST compared to values before the snowstorm (Figure 2(c)).

From December to February, the SST in the study area generally decreases gradually, but the SST drop in 2008 was outstanding relative to the seven years period of 2007–2013 (Figure 2(g)). The average SST variation ranges of the whole study area shown in Figure 2(g) for 2007 (light purple),

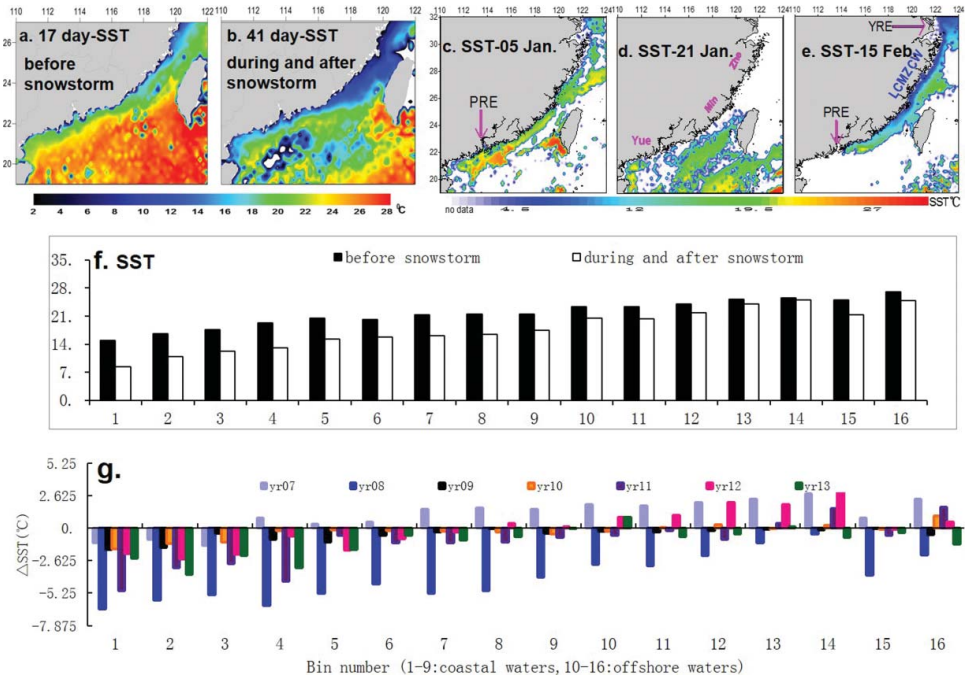

Figure 2. Spatial distribution and change of SST in each bin in the study area before and after the 2008 snowstorm. (a) Spatial distribution of SST before the snowstorm (from 25th December 2007 to 10th January 2008); (b) during and after the snowstorm (from 11th January to 20th February 2008); (c–e): Spatial distributions of SST on 5th January (2c), 21th January (2d) and 15th February (2e) 2008; (f) SST of each bin in the study area before (black), during and after (blank) the snowstorm. Coastal waters: Bins 1–9; offshore waters: Bins 10–16 and (g) change of SST in each bin from December 25 to January 10 ('before') and 11th January to 20th February ('after') in the seven years of 2007–2013. Units: °C. To view this figure in colour, please see the online version of the journal.
Note: $\triangle SST = SST_{after} - SST_{before}$ (Bins 1–9: coastal waters; Bins 10–16: offshore waters).

2008 (blue), 2009 (black), 2010 (yellow), 2011 (deep red), 2012 (pink) and 2013 (green) were 1.06, −3.99, −0.55, −0.28, −1.19, −0.03, and −1.14 °C, respectively.

The MDA-SST in the coastal waters of the study area from 11th January to 20th February 2008 was the lowest in the 14-year period from 2000 to 2013 (Figure A1(a–n)). The TWS was a low-temperature zone, while the south end of the LZS was a high-temperature zone every year. The sizes of the low-temperature and high-temperature zones were clearly and visibly different from year to year. The low-temperature zone in 2008 was more prominent in size and degree than that in the other years, indicating a sharper SST decrease than in all the other years. In the coastal waters, the MDA SST over the 14 years period was 16.19 °C, compared to only 14.19 °C in 2008 with a relatively consistent trend in every Bins (Figure 3). The average SST in the coastal waters in the six years of 2007–2013 (excluding 2008) was 16.72 °C, while it was only 14.19 °C in 2008, with a change of −2.53 °C.

The average temperature in Guangdong province declined greatly from 1st January to 28th February 2008 compared to that in the recent seven years (Figure 4(a)). The average temperature in Guangdong province for the 60-day period from 1st January to 29th February in the seven-year period of 2007–2013 was 14.03 °C, while it was only 11.55 °C in these two months in 2008 (Table 1), representing a drop of −2.48 °C.

3.2. Large discharge of lower temperature water from both PRE and YRE flowing into the NSCS

The discharge of colder PRE diluted water in February 2008 substantially increased and was the largest in the seven-year period, 2006–2012 (Figure 2(c–e)), based on data from Tianhe and Wanshan

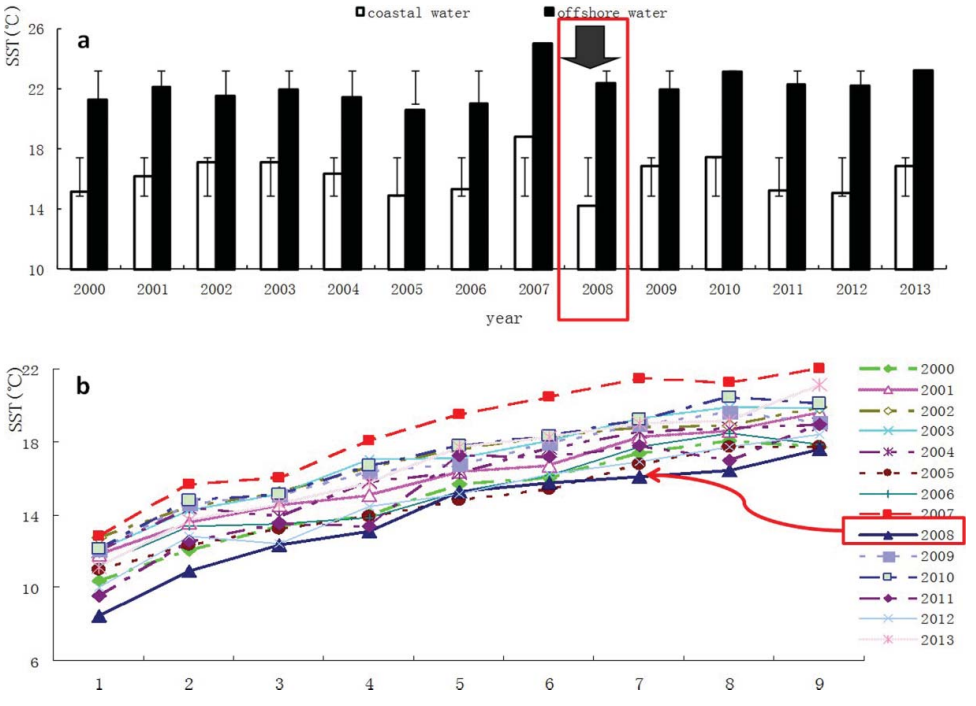

Figure 3. Comparison of SST in coastal and offshore waters, and the change of SST in each bin in the corresponding time period (from 11th January to 20th February). (a) Comparison of SST in the coastal and offshore waters in the corresponding time period in the 14 years of 2000–2013; (b) comparison of SST in each bin in the coastal waters in the 14 years.

hydrometric stations (red and blue dots in Figure 1(b)). The discharge in February 2008 reached 2110 m^3/s, while it was only 1552.67 m^3/s on average in the other seven years, with an increase of 35.90% after the snowstorm. At the same time, the surface water temperature in February 2008 was the lowest of the seven years at only 14.50 °C, 3.32 °C less than the other six-year average.

During 2006–2012, the large discharge with lowest water temperatures in the YRE appeared in January and February 2008 (Figure 5(a,b)). The data were from the Datong hydrometric station. Surface water temperature in the YRE in January and February 2008 was only 6.9 and 5.2 °C, respectively – the lowest in the corresponding period in the recent seven years, or -0.73 and −3.08 °C, compared to the mean surface water temperature of the YRE (a drop of 37.20%). Although the monthly average discharge in January and February 2008 was not the largest among the seven years, the discharges were large enough, at 11,000 m^3/s and 12,200 m^3/s in January and February, respectively, to bring large amounts of colder fresh water with massive suspended sediment and nutrients into the ECS to help form MZCW.

3.3. Chla increase during and after the snowstorm in NSCS

The Chla concentration had a certain increase during and after the freezing rain and snowstorm (Figure 6) in the NSCS. Considering the serious loss of data in Bins 10, 11, 12 and 15 during and after snowstorm, we did not list Bins in Figure 6(c). Except for the blank area, there were more than one hundred thousand valid data points in the study area during and after snowstorm, so the results of MDA-Chla can be well obtained with such a large amount of data. The MDA-Chla in 12 Bins before the snowstorm was 1.45 mg m^{-3} and increased to 1.76 mg m^{-3} after the snowstorm with 24.53% growth rate. The increased rates of Chla were 25.16% and 18.49% in the coastal waters and offshore waters, and a striking increase with 57.70% in Bin 4 and 48.65% in Bin 14, respectively.

The three MODIS Chla images taken on the same dates as the SST images, Figure 2(c), are shown in Figure 6(d–f), and were also the best three single track images in January and February. In the

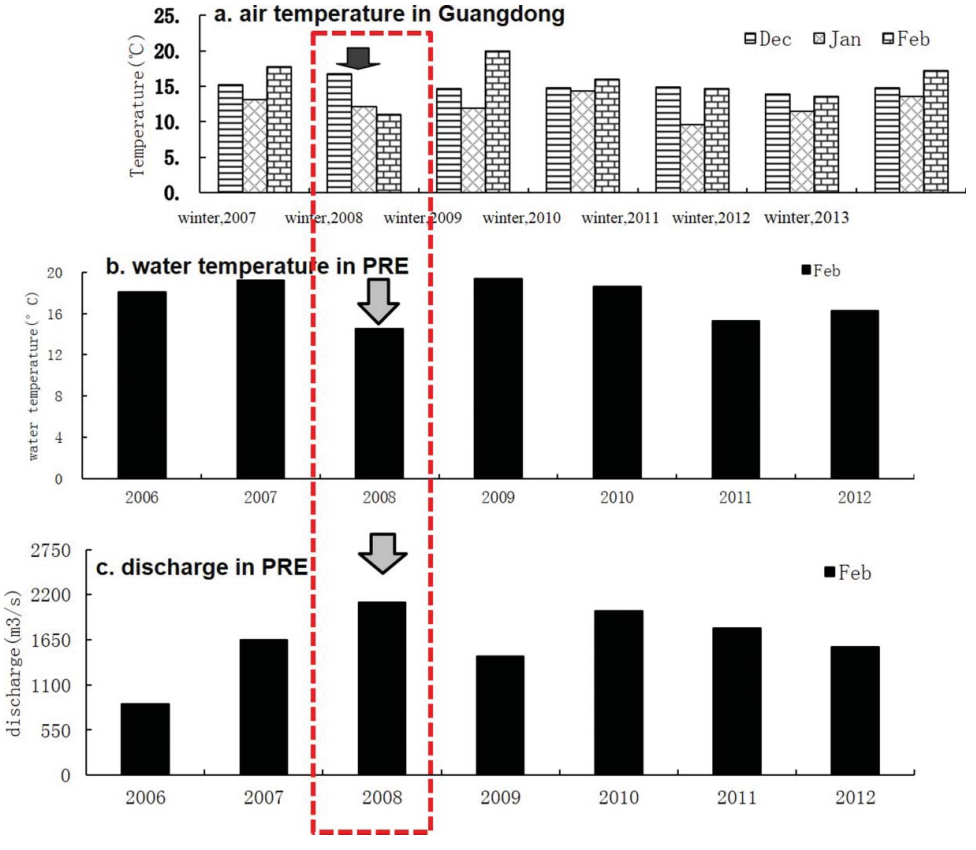

Figure 4. The average temperature in Guangdong, surface water temperature and the discharge from the PRE in recent years, (a) monthly average temperature in Guangdong province adjacent to the NSCS in the seven years of 2007–2013, based on 86 national meteorological stations in Guangdong; black arrow in a, b, c: 2008. (b) and (c) Monthly average temperature of the surface water and discharge at Wanshan and Tianhe Station in the RRE in February from 2006 to 2012.

region southwest of the PRE (indicated by a circle), the Chla on 5th January was only 1.28 mg m^{-3}, while it amounted to 1.47 mg m^{-3} on 21st January (Figure 6(d,e)). In the TWS (marked by a purple prismatic shape), the Chla increased from 1.26 mg m^{-3} on 5th January to 2.08 mg m^{-3} on 15th February , an increase of 65.08% (Figure 6(e,f)). In the LZS region (a blank rectangle), the average Chla concentrations were about 0.37, 0.40 and 0.39 mg m^{-3} on 5th January, 21th January and 15th February, respectively. From these three images of Chla of MODIS from before, during and after the snowstorm, it is apparent that the Chla concentration increased significantly during and after the snowstorm in the NSCS.

3.4. Temporal variation of Chla in the study area

The MDA-Chla concentrations from 11th January to 20th February during 2000–2009 in both coastal and offshore waters of the study area were calculated (Figure 7 and Figure A2). The Chla concentration in the coastal water was much higher than that in the offshore water from 2000 to 2009. The Chla concentration differed greatly in distribution and size from one year to the next, and the Chla concentration in the offshore and coastal waters were 0.67 and 2.18 mg m^{-3} in 2008, respectively, while the MDA-Chla concentration in the same period in the offshore and coastal waters over the 10 years were only 0.55 and 1.76 mg m^{-3}, respectively, with the Chla concentration increasing by 21.63% and 23.86% in the offshore and coastal waters in 2008, respectively (Figure 7 and Figure A2).

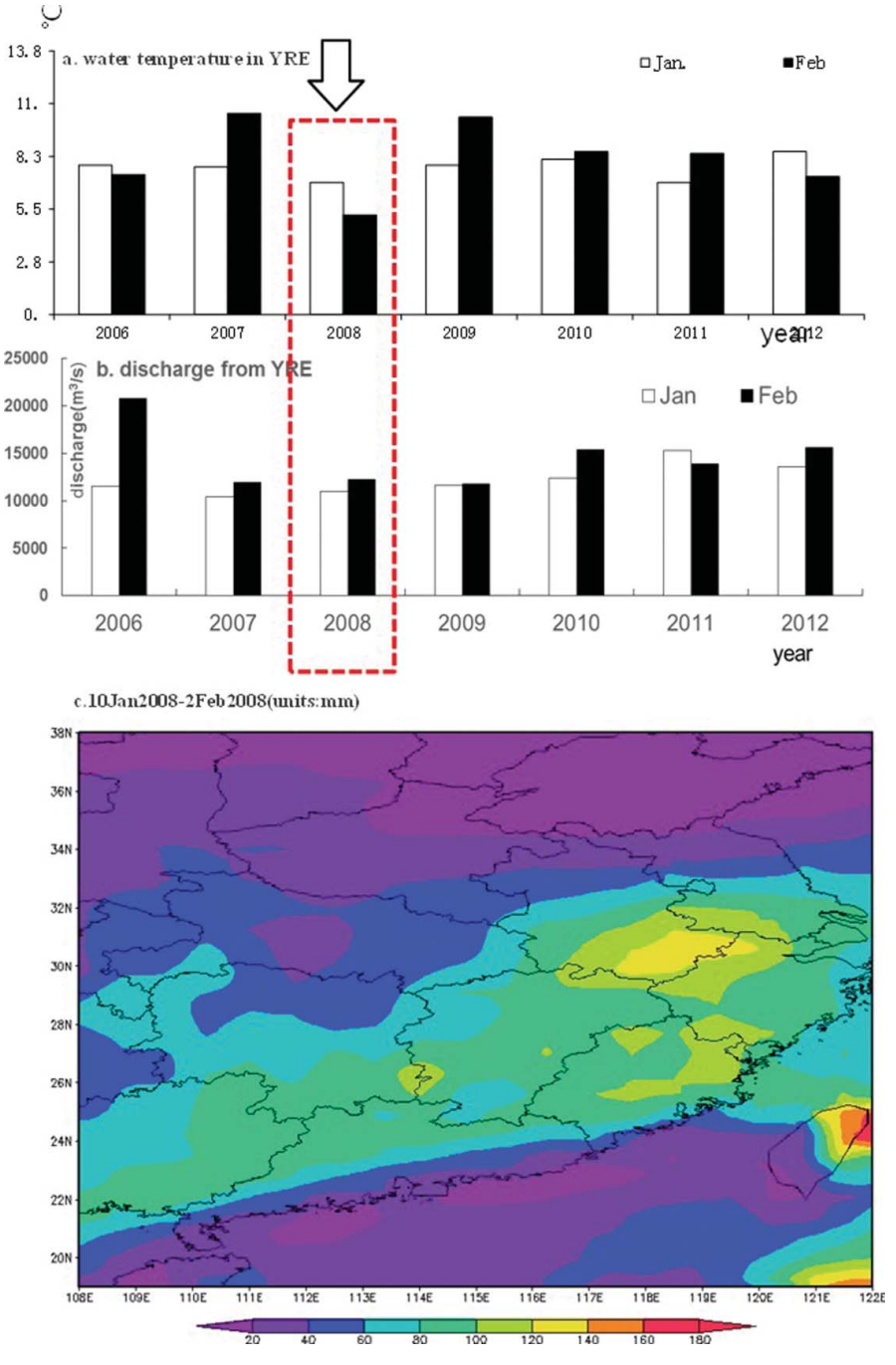

Figure 5. The surface water temperature and discharge at Datong Station in the YRE in January and February from 2006 to 2012. (a) Monthly average temperature of the surface water; (b) Monthly average discharge; and (c) The precipitation in the southeast in China during snowstorm.

Table 1. The average temperature for the 60 day period from January1 to February 29 in Guangdong during 2007–2013.

Years	2007	2008	2009	2010	2011	2012	2013	Comments
Temperature (°C)	15.45	11.55	15.95	15.15	12.15	12.55	15.40	Average temperature of Guangdong
SST (°C)	18.84	14.19	16.90	17.42	15.26	15.09	16.85	SST in coastal waters

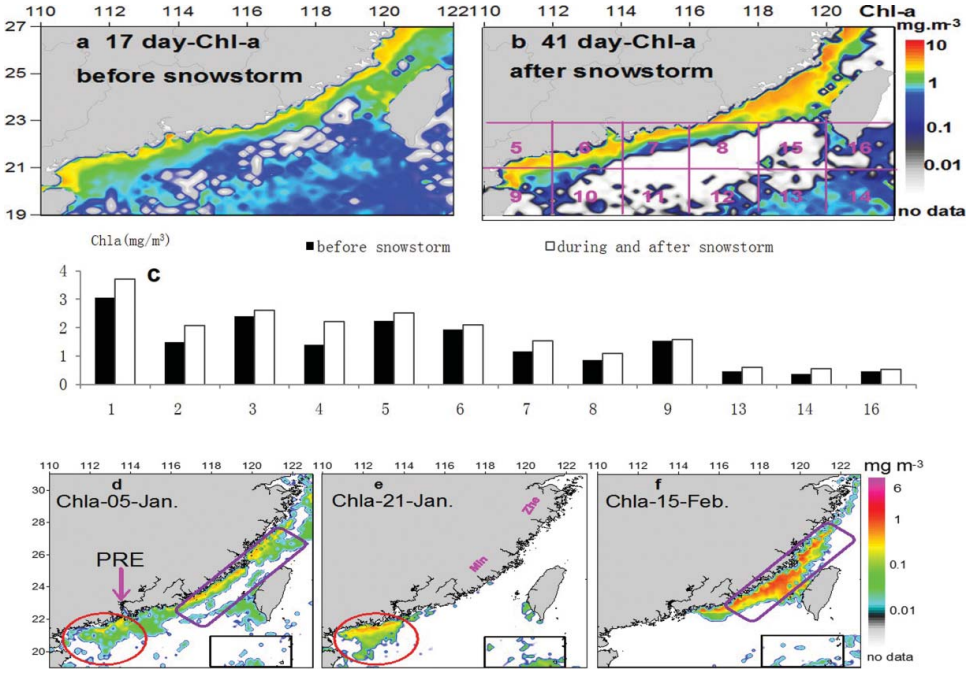

Figure 6. (a–c) Spatial distribution and change of MDA-Chla in each bin in the study area before and after the 2008 snowstorm. (a) Spatial distribution of Chla before the snowstorm; (b) Spatial distribution of Chla during and after the snowstorm; and (c) Chla in each bin in the study area before and after the disastrous winter weather in 2008 (Bins 1–9: coastal waters; Bins 10–16: offshore waters). (d–f) Spatial distribution Chla in single track from January to February in 2008. (d) On 5th January (before snowstorm), (e) 21th January (during snowstorm) and (f) 15th February (after snowstorm). Units: mg/m^3.

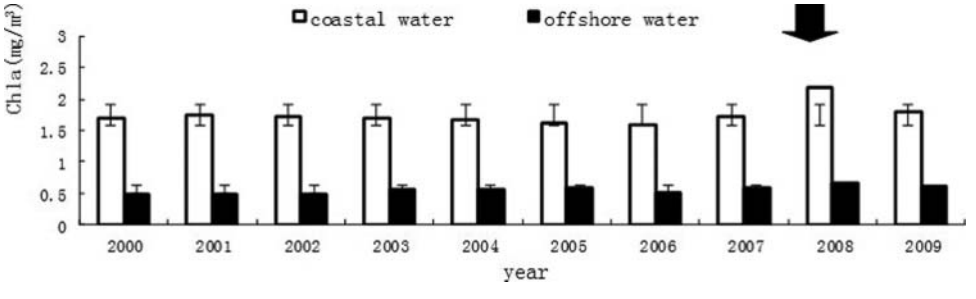

Figure 7. Comparison of MDA-Chla concentration in the nine years of 2000–2009. (a): MDA-Chla concentration in coastal waters (Bins 1–9) and offshore waters (Bins 10–16) in the corresponding time period (from 11th January to 20th February) in the nine years of 2000–2009. Black arrow: 2008. (b) comparison between MDA-Chla concentration in 2008 (hollow) and the Chla concentration in each bin of its climate mean state from 2000–2009 (filled). Units: mg/m^3.

3.5. SSC increase during and after the snowstorm in NSCS

The SSC increased during and after the freezing rain and snowstorm (Figure 8). Although the loss of data in Bins 10–12 was serious during and after the snowstorm due to bad weather, there were plenty of pixels in the whole study area to allow reliable estimates of MDA-SSC. The MDA-SSC in the coastal waters were 48.43 and 83.57 mg/L, while in the offshore waters were 5.60 and 16.50 mg/L before and after the snowstorm, which the increase rates of SSC in the coastal waters and offshore waters were 72.56% and 194.63%, respectively. The striking increases rate with 483.38% in Bin 15

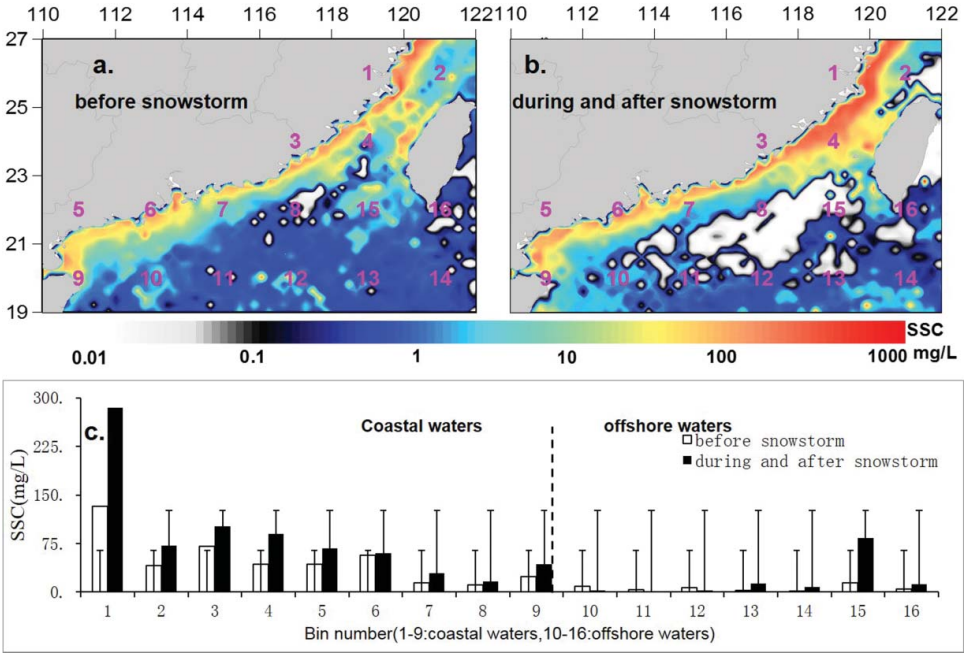

Figure 8. Spatial distribution and change of MDA-SSC in each bin in the study area before and after the 2008 snowstorm. (a) Spatial distribution of SSC before the snowstorm; (b) spatial distribution of SSC during and after the snowstorm; and (c) SSC in each bin in the study area before and after the disastrous weather in 2008 (Bins 1–9: coastal waters; Bins 10–16: offshore waters). Units: mg/L.

near the southwest of TWI, while other bins changed little on average and even decreased in some bins such as 10–12 during and after the snowstorm maybe caused by the much more data loss.

4. Discussion

4.1. Mechanisms for SST reduction during and after the snowstorm in coastal waters

4.1.1. Diluted water from YRE, PRE and their diffusion in winter

The ECS is one of the most productive parts of the world's oceans. The ECS shelf has complex hydrology, as it is affected by the YR discharge, intrusion of the water with about $9.24\times10^{11}m^3$ discharge every year. Usually, of the runoff from YRE, more than 10 000 m^3/s flows to the ECS in winter. In 2008, the discharges from diluted water from YRE reached at 11 000 m^3/s and 12 200 m^3/s in January and February, respectively, which brought larger amounts of colder fresh water with massive suspended sediment and nutrients into the ECS (see Figures 5(a),and 9) and dropped the water temperature in YRE lowest with only 5.2 °C in February from 2006 to 2012(as Figure 5(a)). This colder diluted water turned to the south along the bank of the Zhejiang and formed MZCW by the northeast monsoon as Figure 2(e), which was the same as Pan and Tang (Pan et al. 1997; Tang & Wang 2004). Simultaneously, the discharge from YRE extended offshore and intruded to the southwest (Chang et al. 2009, 2013; Liao et al. 2013; Zhu et al. 2013), mixing with the MZCW and flowing into NSCS as Figure 2(c–e). At the same time, the annual mean discharge of the PRE is about $3.36\times10^{11}m^3$ and is the second largest discharge in China (Pang 2006). The discharge from PRE in February 2008 reached to the top with 2110 m^3/s, with an increase of 35.90% after the snowstorm during 2006–2012 as Figure 4(c). The water temperature in the PRE reached to 14.5 °C during snowstorm, which was the lowest from 2006 to 2012 in February, as given in Figure 4(b). In winter, the diluted water from PRE mainly turns to the southwest by the northeast wind and partly diffuses

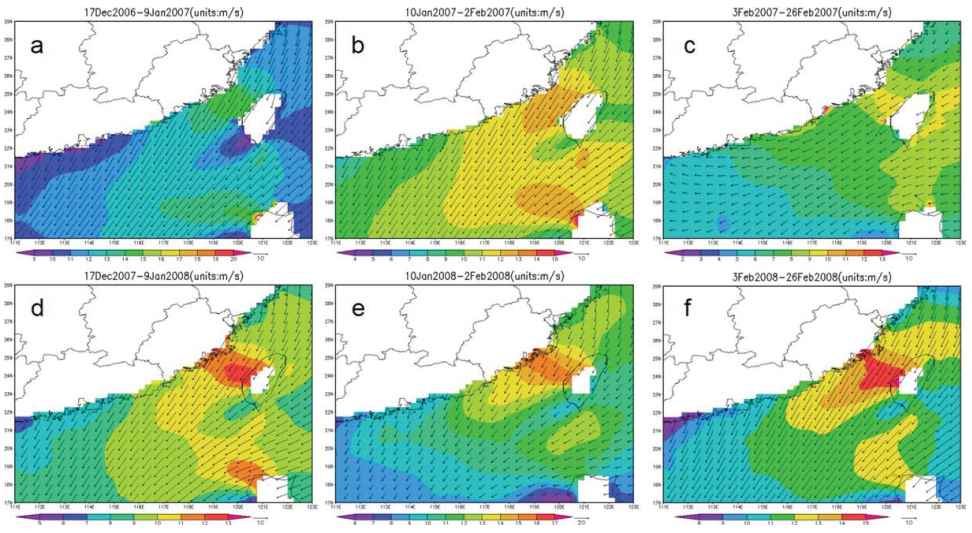

Figure 9. Distribution of monthly average wind from before to after snowstorm. (a) 17 December 2006–9 January 2007, (b) 10 January 2007–2 February 2007, (c) 3 February 2007–26 February 2007, (d) 17 December 2007–9 January 2008, (e) 10 January 2008–2 February 2008, (f) 3 February 2008–26 February 2008. Wind data with a spatial resolution of 0.25°×0.25° and 24 h time interval was obtained from the National Climatic Data Center (NCDC) reanalysis archived by the National Oceanic and Atmospheric Administration (NOAA) (http://rda.ucar.edu/datasets/) and then averaged.

to the east and the shelf area (Lu et al. 2013; Figure 9(a)), bringing lots of suspended sand and nutrients into the NSCS. Controlled by the colder fresh waters from YRE and PRE, the Kuroshio warm current intrusion into the SCS, and southwestward flow and monsoon, the NSCS has a very complex hydrology and dynamic environment (Pang 2006).

4.1.2. *Large colder Min-Zhe coastal waters*

In 2008, surface water temperature in the YRE was the lowest it had been in seven years (Figure 5(a)), and lower compared with the climatological mean surface water temperature of the YRE. Because the precipitation anomalies more than 140 mm were mainly concentrated in the south of the Chain along with the YR and PR, such as Anhui, Zhejiang, Fujian, Jiangxi, Hunan, Guangdong and Guangxi in Figure 5(c) during the snowstorm. The amount of the precipitation in Zhejiang and Fujian close to the research area had a sharp enhancement above their climatological averages over 1971–2000 with 149.7% and 165.5%, respectively (Shi et al. 2010). The discharge from YRE in February 2008 was up to 12,200 m^3/s due to the abundant and persistent rain and heavy snowfall. This colder fresh water from precipitation and dissolved snow converged into the YRE and the coast of the Min-Zhe (Figure 10(a)), just as in our observations in Figure 2: low SST (dark-blue colour) appeared in the northwest of the TWS only before the snowstorm (Figure 2(a)), but after the snowstorm, lower SST occupied the area from YRE to the TWS and stretched southwestward to form a strong oceanic front and temperature gradient (Figure 2(b, d and e)).At the same time, stronger northeastern wind controlled the study area during snowstorm (Figure 9). Combining influence of the cooler discharged water from YRE and the strengthened northeastern winter monsoon in February 2008 promoted a large colder Min-Zhe coastal waters. It was mainly the large colder Min-Zhe coastal waters that drove the SST to drop so remarkably in the coastal water during and after the snowstorm, especially in the TWS.

Shi et al. pointed out that in February of 2008, the overall precipitation in Guangdong and Guangxi provinces during the snowstorm increased with respect to the climatological averages over 1971–2000 by 258.6% and 269.4% respectively (Shi et al. 2010). This precipitation and the dissolved water from the ice and snow formed colder and larger fresh water runoff that pooled mainly into

the PR and intensified the discharge of the PRE, as can be confirmed by noting that the largest discharge with the lowest temperature from PRE for the period 2006–2012 occurred in February 2008 after the snowstorm (Figure 4(b,c)). The larger and colder PRE diluted water flowed into NSCS, whose intrusion of larger and colder PRE diluted water extended mainly to the southwest and partly to the southeast (Hong et al. 2011a; Lu et al. 2013). This larger and colder PRE diluted water and its extension caused the SST to decline further in the study area, especially in the coastal waters near the PRE (Figure 4(b)).

4.1.3. Strong sea–land–air interaction after snowstorm

In January and February 2008, Guangdong coast was dominated by a low temperature anomaly (with respect to the climate norm), while the SST of the coastal waters was close to the average climate temperature (Figure 4(a)). A highly consistent relation can be shown between the average temperature for the 60-day period from 1st January to 29th February of Guangdong and the SST of the coastal waters in the study area (Table 1), with a correlation coefficient of 0.88; these temperatures had no relation to the SST in the offshore waters, however. The average temperature in Shenzhen City in January of a La Nina year (2007/2008 was a typical La Nina year) is 0.4 °C lower than that in the corresponding period over the 30 years climatology (1953–1982) (Yang et al. 2007). We find both the average temperature from January to February in Guangdong province and the average SST after the snowstorm in the coastal waters in 2008 to be lower than the average temperatures in the corresponding period in the recent 30 years climatology (Yang et al. 2007). At the same time, the average temperature anomaly during the snowstorm in the 13 provinces/cities of China (including Shanghai, Zhejiang, Hunan, Guangxi, Guangdong and so on) was −2.83 °C compared with the same period from 1971 to 2000 (Shi et al. 2010, Table 2). Nicholas et al. (2015) pointed out that the land points that are closer to the ocean would be more strongly linked to the nearby SST variability. However, the differences in the land/sea contrast may also reflect differences in physical interactions between land and oceans. The cold ground, as well as the melting snow and ice in most parts of Southeast China, changed the evaporation and heat transfer of surface water, affected sea–land interaction (SLI) and kept low temperatures in Southeast China during the melting snow in February 2008. This indicates that the lower land temperatures in the early part of 2008 strengthened the SLI and the dropped SST of the NSCS.

The monthly average SST of coastal and offshore waters in the study area demonstrated evident interannual variability in the recent 11 years (Figure A3(a,b)). The periodicity of the monthly average temperature difference between offshore and coastal waters is even more remarkable. The temperature difference is larger in winter and smaller in summer, and is largest in February and August. The peak of the temperature difference between offshore and coastal waters in February 2008 was up to 8.72 °C (Figure A3(b)), consistent with in situ measurements (Chang et al. 2009, 2013). It indicates that the impact of land low temperature on the SST in the study area was stronger in winter, and even stronger in the coastal waters than in the offshore waters due to strong SLI. Analysis of hydrometeorological buoy data also shows that the lowest monthly average air temperatures and SST in the TWS for the years 2007–2012 occurred in February 2008 (Li 2013). Thus, the local sea–air interaction was an important factor of SST decrease in the TWS during the cold air outbreaks.

The snowstorm in Southern China might be caused by the 2007 La Nina event (Zheng et al. 2008), and our present study indicates that the strong sea–land–air interaction caused by the cold land and air during and after the snowstorm was one of the important factors that promoted the SST to drop in the north SCS, especially in the coastal waters (Figure 2(c)).

4.1.4. Wind changes modestly in 2008

From before to after snowstorm in 2008, as well as in the corresponding period in 2007, the study area and its adjacent area are controlled by the East Asian monsoons, with prevailing northeasterly

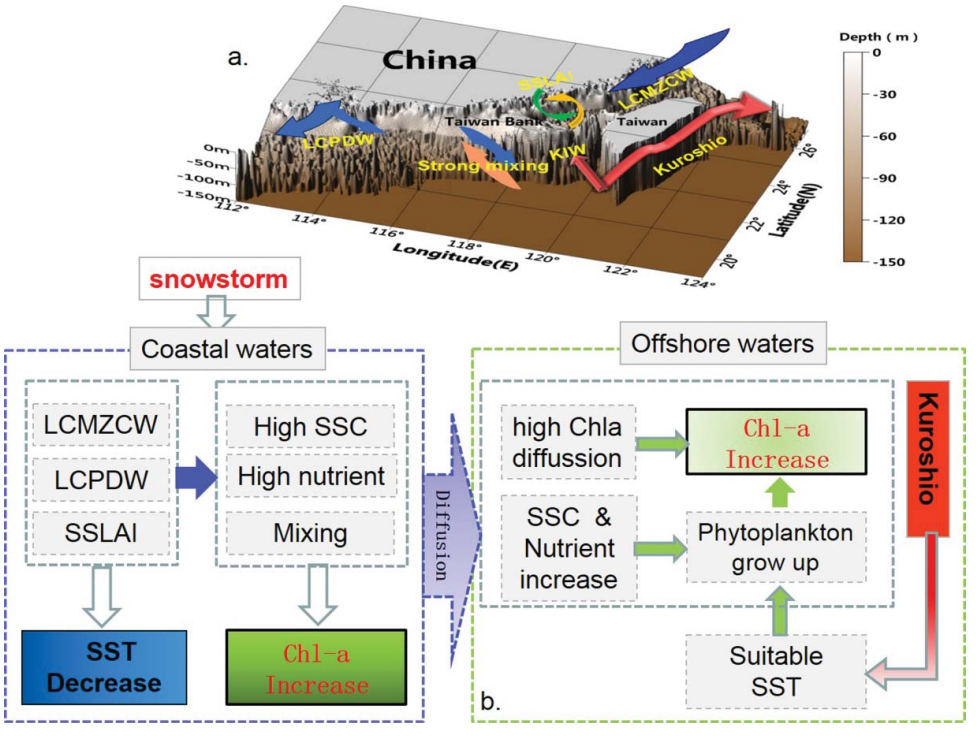

Figure 10. A sketch of the mechanisms controlling SST and Chla concentrations in the study area in response to the 2008 snowstorm: big and dark blue arrow near to YRE: LCMZCW (large colder Min-Zhe coastal waters); Blue arrow near to PRE: LCPDW (larger and colder PRE diluted water); Pair of green and yellow arrows: SSLAI (strong sea-land-air interaction); Light red arrows on the right: KIW (the Kuroshio intrusion water from LZS); Light blue arrow and light orange arrow in the middle: SVM (strong vertical mixing). To view this figure in colour, please see the online version of the journal

wind in winter (shown in Figure 9(a–f)). From before to after snowstorm, direction of the wind changed only slightly, while the max wind speed increased from 12 to 17 m/s, which was larger than that in 2007, especially in the TWS. The SST in the study area was much higher than that in 2008 (see Figure A1(h,i)). The article (Price et al. 1986) mentioned that the process of diurnal cycle plays an important role in shaping the long-term response of the upper ocean to atmospheric forcing. The trapping depth of the thermal and velocity response is proportional to wind speed (τ), and inversely proportional to the surface heat flux ($Q^{1/2}$). Meanwhile, changes in the mixed layer depth were directly related to atmospheric forcing, and then the upper ocean temperature gradient was forced to change (Cisewski et al. 2005). Then, the strong wind in winter can cause greater vertical mixing, lower SST and larger productivity in the ocean (Tang et al. 2004b; Hong et al. 2011b; Shang et al. 2012). With the lower temperature and stronger wind during snowstorm especially in the TWS (as in Figures 2, 5(c), 9(d–f) and A1), the vertical mixing become greater and trapping depth become deeper, which promoted larger productivity in the ocean.

According to the above observations and analysis, the mechanisms for the significant SST decline after the 2008 snowstorm in the study area, especially in the coastal waters, include mainly the following (Figure 10). On the one hand, the large colder Min-Zhe coastal waters and larger and colder PRE diluted water from the large infusion of cold fresh water after the snowstorm caused the remarkable SST drops in the coastal water, especially the sharp drops in the TWS. On the other hand, stronger monsoon and sea–land–air interaction in winter, especially during and after the snowstorm in the coastal waters, caused SST to decline further.

Table 2. Averaged air temperature for the most significantly impacted provinces and special districts during China's great snowstorms of 2008 (10th January–2nd February 2008). Anomalies are calculated against a region's climate records during the same period (the climatology is the average over 1971–2000 (Shi et al. 2010)). SH: Shanghai, JS: Jiangshu, ZJ: Zhejiang, AH: Anhui, JX: Jiangxi, HeN: Henan, HB: Hebei, HN: Hunan, CQ: Chongqing, GZ: Guizhou, FJ: Fujian, GD: Guangdong and GX: Guangxi.

Province	SH	JS	ZJ	AH	JX	HN	HeB	HN	CQ	GZ	FJ	GD	GX
Temperature (°C)	2.8	0.1	3.5	−1.2	1.4	−2.9	−0.7	−0.5	2.8	0.7	7.8	10.3	7.0
Anomaly (°C)	−0.9	−0.5	−1.0	−2.9	−3.8	−3.2	−3.8	−4.9	−3.1	−4.1	−1.0	−2.4	−4.2

4.2. The cause for SSC increase during and after the snowstorm in the study area, especially in offshore waters

Suspended sediment is an important parameter of water quality. Scattering and absorption of light by the suspended particles reduce the penetration into the water of photosynthetically available radiation (PAR) for benthic plants (Davies, R J et al. 1992). Fine sediment increased water turbidity, limiting light intensity. The chemisorption of the sand particle impacts the marine biogeochemistry process of the coastal waters, thus indirectly affecting primary productivity. There are about 4.175×10^8 t/a sediment loads from YRE (Wang et al. 2006), whereby large amounts of terrestrial detritus, suspended sediments, nutrients and pollutants are carried to the continental ECS with intrusion and diffusion of MZCW (Milliman et al. 1985; Wang et al. 2003; Yuan et al. 2008; Bian 2012; Fu et al. 2014). Lee and Chough (1989) and Jian (2006) pointed out that more than half of the sediment discharge of YRE was carried to the Min-Zhe coastal waters. There was about 2.4×10^8 t/a sediment deposition in the Min-Zhe coastal area (Liu et al. 2007). In winter, the diffusion and intrusion of the sediments from YRE are carried out by the monsoon, even to the NSCS through TWS and to open sea areas (Yuan et al. 2008; Bian 2012), which was the same as our results as in Figure 8(a,b). The SSC were much higher in Bin 1 located in the Min-Zhe coastal water than in other bins both before and after the snowstorm (Figure 8(c)). With the increase of the runoff from the precipitation and melted snow during and after the snowstorm (as in Figures 4–5), large amounts of sediments were carried into the study area from the YRE and PRE, significantly increasing the SSC during and after the snowstorm (as in Figure 10).

In the offshore waters, there was a much higher increase rate of MDA-SSC than in the coastal waters during and after the snowstorm. Although the increase rate was up to 194% in SSC in the offshore waters, the absolute increment of SSC was only 11.73 mg/L, only about 30% with that in the coastal waters.

First, the discharge from YRE extended offshore and intruded to the southwest (Chang et al. 2009, 2013; Liao et al. 2013; Zhu et al. 2013), mixing with the MZCW and flowing into NSCS, as given in Figure 2(c–e). From before to after snowstorm, the larger runoff from YRE and PRE caused by the heavy rainfall and melting snow and ice (as in Figure 5(c)) and stronger northeast monsoon (Figure 9) would lead to much diffusion of the cold water with high SSC in the coastal waters to the offshore waters, while much stronger diffusion and advection would carry large amount of sand from the coast to the offshore, which promoted the increase of SSC in the offshore waters.

Second, the increase of SSC in the offshore waters caused by snowstorm is mostly in Bins 13–15, especially in Bin 15, where following the snowstorm, the SSC increased to 5.83 times its pre-storm value (Figure 8(c)). The unique location of Bin 15 at the TW bank (southwest of TW) with only about 30 m depth and where the cold water from the west and warm water from the southeast converge (Hu & Muller-Karger 2007; Fang et al. 2010) should be accounted for the increase of the SSC. Two possible mechanisms may induce the high increased SSC in Bin 15.On the one hand, this bin is relatively near the mainland, from before to after snowstorm, the much greater monsoon mainly concentrated the TWS (as in Figure 9(d–f)) would enhance southward flow from MZCW carrying suspended sediment from mainland China (Bian 2012; Zhu et al. 2013; Wang et al. 2012). On the other hand, strong vertical mixing (SVM) and entrainment in this area caused by stronger northwest monsoon during snowstorm can bring bottom water to the surface, and thereby could cause a re-suspension of the sediment in this bin (Tian et al. 2015), so a significant growth of SSC in Bin 15 would be found in our study. However, in Bins 10–12, there was a little decrease in SSC, maybe due to error from the significant data loss during and after snowstorm.

4.3. The cause for Chla increase during and after the snowstorm in the study area, especially in coastal waters

Nutrients abundance, especially N, P and Si, is one of the factors controlling the growth of phytoplankton in the upper layer of the ocean (Syrett 1953; Bongersch 1956; Foggge 1959; Lewinjc 1962; Brzezinskim 1990). Other factors include the light conditions (Gabric & Parslow 1989) and the water temperature (Eppley 1972; Raven & Geider 1988; Tang et al. 2006; Hao et al. 2007; Li 2013). These factors influence Chla content in water by changing phytoplankton growth, metabolism and other physiological activities. Yang et al. (2007) pointed out that among the factors controlling phytoplankton growth, the most important is nutrients, second is the light and third is the temperature. In winter in the MZCW, nutrient concentrations usually are high, sometimes nitrate concentration can reach up to 35 μmol/L in the MZCW (Wang et al. 2012), and the stratification is weak due to the SVM by the northwest monsoon (Figure 9) during snowstorm, which can bring the nutrients to the upper layer from deep layers and even from the bottom (Tang et al. 1998; Li et al. 2000; Liao et al. 2013). During and after the snowstorm in 2008, we observed oceanic fronts with large temperature gradients in the TWS and LZS caused by the large colder Min-Zhe coastal waters, larger and colder PRE diluted water and sea–land–air interaction, respectively (Figures 2(b, d, and e) and 4(b,c)). With the strong extension of the fresh water, front and SVM, higher SSC in the study area during and after snowstorm indicated that abundant nutrients were carried into the upper layer of the ocean, especially in the coastal waters. These nutrients promoted the growth of phytoplankton and enhanced the concentration of the Chla (Figure 10).

Light is an important factor for phytoplankton growth, but phytoplankton can also adapt to the intensity of the light by changing intracellular pigment or photosynthetic enzyme (Odum & Wilson 1962). Maucha pointed out that the light intensity is enough for the phytoplankton to assimilate on the surface of the water at any point on Earth (Maucha et al. 1948). Although SSC and turbidity increased, while the transparency decreased during and after the snowstorm, the light was not a limiting factor for phytoplankton growth in the study area.

In the offshore waters, comparing with before or 10-year average, Chla during and after the snowstorm increased a little less than that in coastal waters. The increase mainly happened in the 13–14 and 16 Bins (as Figure 6(b,c)), while other bins in the offshore waters changed uncertainly may be caused by the missing data. The growth mechanism maybe different with that in the coastal waters (for the serious data loss, the discussed did not include bins of 10–12 and 15). On the one hand, with the larger colder Min-Zhe coastal water and larger and colder PRE diluted water (as in Figure 2(b) and 6(b)), as well as higher levels of diffusion, the entrainment and advection by the stronger northwest monsoon (as in Figure 9) during snowstorm, the terrestrial debris (sediment) from the coastal waters would bring the higher SSC and nutrients to the offshore waters, which would been seen from higher increase rate in SSC more than 400% in Bins 13, 14 and 15 (as in Figure 8). The abundant nutrients carried from SSC would promote the growth of phytoplankton and enhance the concentration of the Chla further (as in Figure 10(b)). At the same time, the higher Chla concentration could spread and transport outward and southward with the diffusion of the MZCW and southwest flow of TWS, which could directly raise the concentration of Chla during and after snowstorm. On the other hand, the higher nutrients and Chla in the subsurface would be brought to the surface under the strong mixing caused by the stronger northwest monsoon during snowstorm (as in Figure 9), which was beneficial to the rising of Chla in the offshore waters (Ma et al. 2013).

Temperature higher than 15 °C is suitable for the growth of many kinds of common phytoplankton, while the optimal temperature for growth is about 20–25 °C (Behrenfeld et al. 1997; Tang et al. 2006; Chai et al. 2009). SST did not decrease much in Bins 13, 14 and 16 because they are located near the LZS, where were influenced by the Kuroshio warm water westward flow (red arrows in Figure 10) to this sea area (about 119°E, 20°N) in winter (Metzger & Hurlburt 1996; Liang et al. 2008, Hong et al. 2011a; Chang et al. 2009, 2013; Liao et al. 2013). Mainly due to the contribution of the Kuroshio intrusion water (KIW) (as Figure 10), suitable temperature with average value of 22.42 °C in the offshore waters after the snowstorm provided favourable environment for the growth of phytoplankton, which would be beneficial for the further elevation of Chla.

5. Summary

A severe weather event with wide-range sustained low-temperature, freezing rain and sleet took place in Southern China in 2008 had profound effects on the marine environment in the NSCS and TWS:

(1) During and after the 2008 snowstorm, the SST in the NSCS and TWS sharply dropped, especially in the coastal waters, while the SSC and Chla concentrations increased remarkably, compared to their values before the snowstorm and to climatology, especially in the coastal waters and TWS.
(2) The great drop in SST in the coastal waters was likely influenced by the large infusion of colder Min-Zhe coastal waters and diluted water from the PRE, as well as by the strong sea–land–air interaction during and after the snowstorm.
(3) The large increment in SSC in NSCS mainly came from transport and entrainment from large colder Min-Zhe coastal waters, larger and colder PRE diluted water and their diffusion to the southeast by the monsoon, while the increase of Chla concentration is related to abundant nutrients supply from YRE and PRE, mixing and front in the coastal waters, while in the offshore waters, a strong transport and extension of MZCW with high SSC, nutrient and Chla, as well as suitable temperature, which promoted the increase of Chla.

Acknowledgements

This study was supported by the National Marine Important Charity Special Foundation of China (201305019), the NSFC (41340049, 41430968), Collaborative Innovation Center for 21st-Century Maritime Silk Road Studies, China (2015HS05), Visiting Fellowship Program (to Gad Levy and DL Tang) of State Key Laboratory of Tropical Oceanography (2015), Chinese Academy of Sciences (2013T1Z0048), and High-end Foreign Experts Recruitment Program, Guangdong (GDJ20154400004); Natural Science Foundation of Guandong Provience (2014A030313603); Science and Technology Planning Project of Guangdong (2013B030200002, 2016A020222016);

Project of Enhancing School with Innovation of Guangdong Ocean University (GDOU2014050226). The land temperature data was supplied by Guangdong Meteorological Service (http://www.grmc.gov.cn/). The PRE discharge data and the surface water temperature data of YRE were supplied by the Pearl River (http://www.pearlwater.gov.cn/) and Changjiang Water Resources commission of the Ministry of Water Resources; (http://www.cjw.com.cn/). Meanwhile, thanks for guidance of academician Pan Delu of Second Institute of Oceanography, State Oceanic Administration and thank our colleagues for their input.

Disclosure statement

No potential conflict of interest was reported by the authors.

Funding

National Marine Important Charity Special Foundation of China [grant number 201305019]; NSFC [grant number 41340049], [grant number 41430968]; Collaborative Innovation Center for 21st-Century Maritime Silk Road Studies, China [grant number 2015HS05]; Visiting Fellowship Program (to Gad Levy and DL Tang) of State Key Laboratory of Tropical Oceanography [grant number 2015]; Chinese Academy of Sciences [grant number 2013T1Z0048]; High-end Foreign Experts Recruitment Program, Guangdong [grant number GDJ20154400004]; Natural Science Foundation of Guandong Provience [grant number 2014A030313603]; Science and Technology Planning Project of Guangdong [grant number 2013B030200002], [grant number 2016A020222016]; Project of Enhancing School with Innovation of Guangdong Ocean University [grant number GDOU2014050226].

References

Babin SM, Carton JA, Dickey TD, Wiggert JD. 2004. Satellite evidence of hurricane-induced phytoplankton blooms in an oceanic desert. J Geophys Res: Oceans. 109:325–347.

Bao XW, Wan XQ, Gao GP, Wu DX. 2002. The characteristics of the seasonal variability of the sea surface temperature field in the Bohai Sea, the Huanghai Sea and the East China Sea from AVHRR data. Acta Oceanol Sin. 24:125–133.

Behrenfeld MJ, Falkowski PG. 1997. Photosynthetic rates derived from satellite – based chlorophyll concentration. Limnol Oceanogr. 42:1–20.
Bian CM. 2012. [Chinese coastal sediment transport in the Bohai Sea Yellow Sea and East China Sea]. Qingdao: Ocean University of China; p. 1–112. Chinese.
Bongersch HJ. 1956. Aspects of nitrogen assimilation by cultures of greenalgae (Chlorella vulgaris, strain A and S cenedesmus). Meded Land Bouwhogesch Wageningen. 56:1–52.
Brzezinskim A, Olsonrj CS. 1990. Silicon availability and cell-cycle progression in marine diatoms. Mar Ecol Prog Ser. 67:83–96.
Chai C, Yu Z, Shen Z, Song X, Cao X, Yao Y. 2009. Nutrient characteristics in the Yangtze River Estuary and the adjacent East China Sea before and after impoundment of the Three Gorges Dam. Sci Total Environ. 407:4687–4695.
Chang Y, Lee KT, Lee MA, Lan KW. 2009. Satellite observation on the exceptional intrusion of cold water in the Taiwan Strait. Terr Atmos Oceanic Sci. 20.
Chang Y, Lee MA, Lee KT, Shao KT. 2013. Adaptation of fisheries and mariculture management to extreme oceanic environmental changes and climate variability in Taiwan. Mar Policy. 38:476–482.
Chu PC, Lu S, Chen Y. 1997. Temporal and spatial variabilities of the South China Sea surface temperature anomaly. J Geophys Res Oceans (1978–2012). 102:20937–20955.
Cisewski B, Strass VH, Prandke H. 2005. Upper-ocean vertical mixing in the Antarctic Polar Front Zone. Deep Sea Res Part II. 52:1087–1108.
Davies R, Younger A, Chapman R. 1992. Water availability in a restored soil. Soil Use Manage. 8:67–73.
Eppley. 1972. Temperature and phytoplankton growth in the sea. Fish Bull. 70:1063–1085.
Fang JY, Chen J, Hu Y, Liao LZ. 2010. Types of settling particulate matter and flocs around the Taiwan Shoal. J Trop Oceanogr. 29:48–55.
Foggge. 1959. Nitrogen nutrition and metabolic patterns in algae. Symp Soc Exp Biol. 13:106–125.
Fu DY, Luan H, Pan DL, Zhang Y, Wang LA, Liu DZ, Ding YZ, Li X. 2016. Impact of two typhoons on the marine environment in the Yellow Sea and East China Sea. Chin J Oceanol Limnol. 34:871–884.
Fu DY, Pan DL, Ding YZ. 2009. [Quantitative study of effects of the sea chlorophyll-a concentration by typhoon based on remote sensing]. Acta Oceanolog Sin. 31:46–56. Chinese.
Fu DY, Pan DL, Wang DY, Zhang Y, Ding YZ, Liu DZ. 2014. The analysis of phytoplankton blooms off the Yangtze River Estuary in the spring of 2007. Aquatic Ecosyst Health Manag. 17:221–232.
Gabric A, Parslow J. 1989. Effect of physical factors on the vertical distribution of phytoplankton in eutrophic coastal waters. Mar Freshwater Res. 40:559–569.
Gao H, Chen LJ, Jia XL, Ke ZJ, Han RQ, Zhang PQ, Wang QY, Sun CH, Zhu YF, Li Wet al., 2008. [Analysis of the severe cold surge, Ice—snow and frozen disasters in South China during January 2008:II. Possible climatic causes]. Meteorol Mon. 34:101–106. Chinese.
Hao Q, Ning XR, Liu CG, Cai YM, Le FF. 2007. Satellite and in situ observations of primary production in the northern South China Sea. Acta Oceanolog Sin. 129:58–68.
He X, Bai Y, Chen C-TA, Hsin Y-C, Wu C-R, Zhai W, Liu Z, Gong F. 2014. Satellite views of the episodic terrestrial material transport to the southern Okinawa Trough driven by typhoon. J Geophys Res Oceans. 119:4490–4504. doi:10.1002/2014JC009872.
Hong HS, Chai F, Zhang CY, Huang BQ, Jiang YW, Hu JY. 2011a. An overview of physical and biogeochemical processes and ecosystem dynamics in the Taiwan Strait. Cont Shelf Res. 31:S3–S12. doi:10.1016/j.csr.2011.02.002
Hong HS, Liu X, Chiang KP, Huang BQ, Zhang CY, Hu J, Li YH. 2011b. The coupling of temporal and spatial variations of chlorophyll a concentration and the East Asian monsoons in the southern Taiwan Strait. Cont Shelf Res 31:S37–S47.
Hu C, Muller-Karger FE. 2007. Response of sea surface properties to Hurricane Dennis in the eastern Gulf of Mexico. Geophys Res Lett. 34:248–265.
Jian H. 2006. Measur ements and analysis of water discharges and suspended sediment fluxes in Changjiang Estuary. Acta Geogr Sinica. 26:35–47.
Lan YC, Lee MA, Liao CH, Lee KT. 2009. Copepod community structure of the winter frontal zone induced by the Kuroshio branch current and the China coastal current in the Taiwan Strait. J Mar Sci Technol. 17:1–6.
Lee HJ, Chough SK. 1989. Sediment distribution, dispersal and budget in the Yellow Sea. Mar Geol. 87:195–205.
Lewinjc. 1962. Physiology and biochemistry of the Algae[C], London: Academic Press.
Li T. 2013. [Analysis of temporal and spatial characteristics of sea surface chlorophyll-a concentrations in Northern South China Sea based on long-time series remote sensing data and EOF method]. WuHan: China University of Geosciences; p. 1–64. Chinese.
Li L, Guo XG, Wu RS. 2000. [Oceanic fronts in southern Taiwan Strait]. J Oceanogra Phyin Taiwan Strait. 19:147–156. Chinese.
Liang WD, Yang YJ, Tang TY, Chuang WS. 2008. Kuroshio in the Luzon Strait. J Geophys Res: Oceans. 113:2092–2112.
Liao EH, Jiang YW, Li L, Hong HS, Yan XH. 2013. The cause of the 2008 cold disaster in the Taiwan Strait. Ocean Model. 62:1–10.
Liu DZ, FU DY, Shen CY, Xu B. 2010. [Study advances on remote sensing of suspended sediment in estuaries and coastal case 11 water]. Marine Environ Sci. 29:611–616. [Chinese].

Liu DZ, Fu DY, Xu B, Shen CY. 2012. Estimation of total suspended matter in the Zhujiang (Pearl) River estuary from Hyperion imagery. Chin J Oceanol Limnol. 30:16–21.
Liu KK, Peng TH, Shaw PT, Shiah FK. 2003. Circulation and biogeochemical processes in the East China Sea and the vicinity of Taiwan: an overview and a brief synthesis. Deep Sea Res Part II. 50:1055–1064.
Liu J, Xu K, Li A, Milliman JD, Velozzi DM, Xiao S, Yang Z. 2007. Flux and fate of Yangtze river sediment delivered to the East China Sea. Geomorphol. 85:208–224.
Lu LY, Zhan JM, Geng BX. 2013. [Study of the Pearl River plume dispersion based on flux budget analysis]. Chinese J Hydrodynam. 28:252–259. Chinese.
Ma AH, Liu XN, Li T, Liu ML. 2013. The satellite remotely sensed analysis of the temporal and spatial variability of chlorophyll a concentration in the northern south china sea. Acta Oceanolog Sin. 35:98–105.
Ma XG. 2009. [Diagnosis of catastrophic freezing rain and sleet in January 2008 in the southern China]. J Meteorol Environ. 25:24–26. Chinese.
Maucha R. 1948. Die photosynthese des phytoplanktons vom gesichtspunkte der quantenlehre. Hydrobiologia. 1:45–62.
Metzger EJ, Hurlburt HE. 1996. Coupled dynamics of the south China sea, the Sulu sea, and the Pacific ocean. J Geophys Res Oceans (1978–2012). 101:12331–12352.
Milliman JD, Beardsley RC, Yang Z, Limeburner R. 1985. Modern huanghe-derived muds on the outer shelf of the East China Sea: identification and potential transport mechanisms. Cont Shelf Res. 4:175–188.
Nicholas L, Tyrrell D, Claudia F, Scott W, Mike R. 2015. The influence of global sea surface temperature variability on the large-scale land surface temperature. Clim Dyn. 44:2159–2176.
Odum HH, Wilson R. 1962. [Further studies on reaeration and metabolism of Texas bays, 1958–1960]. Texas: Publications of the Institute of Marine Science. Chinese.
Pan Y, Wang K, Huang S. 1997. [Analysis on the path of transportation and diffusion of Changjiang diluted water]. Dong Hai Marine Sci. 15:25–34. Chinese.
Pang HL. 2006. [Analysis of diffuse route of the Zhujing river diluted water]. QingDao: Ocean University of China. Chinese.
Price JF, Weller RA, Pinkel R. 1986. Diurnal cycling: Observations and models of the upper ocean response to diurnal heating, cooling, and wind mixing. J Geophys Res Oceans. 91:8411–8427.
Raven JA, Geider RJ. 1988. Temperature and algal growth. New Phytol. 110:441–461.
Shang SL, Li L, Li J, Li YH, Lin G, Sun J. 2012. Phytoplankton bloom during the northeast monsoon in the Luzon Strait bordering the Kuroshio. Remote Sens Environ. 124:38–48.
Shaw PT, Chao SY. 1994. Surface circulation in the South China Sea. Deep Sea Res Part I. 41:1663–1683.
Shi X, Xu X, Lu C. 2010. The dynamic and thermodynamic structures associated with a series of heavy precipitation events over China during January 2008. Weather Forecasting. 25.
Sipelgas L, Raudsepp U, Kõuts T. 2006. Operational monitoring of suspended matter distribution using MODIS images and numerical modelling. Adv Space Res. 38, 2182–2188.
Syrett PJ. 1953. The assimilation of ammonia by nitrogen-starved cells of Chlorella vulgaris: Part I. The correlation of assimilation with respiration. Annal Bot. 17:19–27.
Tang DL, Di BP, Wei G, Ni IH, Oh IS, Wang SF. 2006. Spatial, seasonal and species variations of harmful algal blooms in the South Yellow Sea and East China Sea. Hydrobiologia. 568:245–253.
Tang DL, Kawamura H, Doan−Nhu H, Takahashi W. 2004a. Remote sensing oceanography of a harmful algal bloom off the coast of southeastern Vietnam. J Geophys Res: Oceans (1978–2012). 109:1–7.
Tang DL, Kester DR, Ni I, Kawamura H, Hong HS. 2002. Upwelling in the Taiwan Strait during the summer monsoon detected by satellite and shipboard measurements. Remote Sens Environ. 83:457–471.
Tang DL, Ni IH, Müller-Karger FE, Liu ZJ. 1998. Analysis of annual and spatial patterns of CZCS-derived pigment concentration on the continental shelf of China. Cont Shelf Res. 18:1493–1515.
Tang DL, Ni IH, Müller-Karger FE, Oh IS. 2004b. Monthly variation of pigment concentrations and seasonal winds in China's marginal seas. Hydrobiologia, 511:1–15.
Tang X, H, Wang F. 2004. [Analyses on hydrographic structure in the Changjiang River Estuary adjacent waters in Summer and Winter]. QingDao: Studia Marina Sinica; p. 42–66. Chinese.
Tassan S, Ferrari GM. 2003. Variability of light absorption by aquatic particles in the near-infrared spectral region. Appl Opt. 42:4802–4810.
Tian P, Zhai J, Zhao G, Mu X. 2015. Dynamics of runoff and suspended sediment transport in a highly erodible catchment on the Chinese loess plateau. Land DegradDev. doi:10.1002/ldr.2373.
Wang DX, Du Y, Shi P. 2002. [Climatological atlas of physical oceanography in the upper layer of the South Chinese Sea]. Beijing: China Meteorological Press. Chinese.
Wang J, Hong H, Jiang Y, Yan X-H. 2013. Mechanism for initiation of the offshore phytoplankton bloom in the Taiwan Strait during winter: a physical–biological coupled modeling study. Biogeosci Discuss. 10:14685–14714.
Wang L, Lei LZ, XIE YY, Huang BQ. 2012. [A preliminary study on the new prodctivity and primary productivity of Wast China Sea and northern South China Sea in winter]. J Marine Sci. 30:59–66. Chinese.
Wang S, Hassan MA, Xie X. 2006. Relationship between suspended sediment load, channel geometry and land area increment in the Yellow River Delta. Catena. 65:302–314.
Wang YH, Jan S, P WD. 2003. Transports and tidal current estimates in the Taiwan Strait from shipboard ADCP observations (1999-2001). Estuarine Coastal Shelf Sci. 57:193–199.

Yan JY, Chen QJ, Zhang XZ, Huang AF. 1993. China coastal climate. Beijing: China Meteorological Press. Chinese.
Yan Z, Tang D. 2009. Changes in suspended sediments associated with 2004 Indian Ocean tsunami. Adv Space Res. 43:89–95.
Yang DF, Chen ST, Hu J, Wu JP, Huang H. 2007. Magnitude order of the effect to light, water temperature and nutrients on phytoplankton growth. Marine Environ Sci. 26:201–207.
Yang L, Liu DH, Zhong BL. 2007. [Analysis of La Nina effect on local climate]. J Meteorol Res Appl. 1:007. Chinese.
Yuan Y, Wei H, Zhao L, Jiang W. 2008. Observations of sediment resuspension and settling off the mouth of Jiaozhou Bay, Yellow Sea. Cont Shelf Res. 28:2630–2643.
Zheng DW, Lee MS, Huo ZG. 2008. [Effects of 2008 snow disaster in Southern China on agriculture and countermeasures]. J Inst Disaster-Prevention Sci Technol. 10:1–4. Chinese.
Zhu DY, Li L, Guo XG. 2013. Seasonal and interannual variations of surface current in the southern Taiwan Strait to the west of Taiwan Shoals. Chin Sci Bull. 58:4171–4178. doi:10.1007/s11434-013-5907-y.

Appendix

The data fusion of remote sensing for multi-day average (MDA) was done using the algorithm as follows

$$\text{Aver} = \frac{\sum_{j=1}^{m} \frac{\sum_{i=1}^{N} \text{Value}(i)_p}{N}}{m}$$

where *Aver* is the multiple-day-average value of SST/Chl-a/SSC in the study area, m is the number of split windows in the area, and N is the number of remote sensing images involved in the calculation. Value $(i)_p$ represents the current value of point 'p' in the study area, whose number is 'i' (if a pixel is missing, the result is not included). First, an average was calculated for a small bin with dimensions of $2^\circ \times 2^\circ$ as in Figure 2, and then through sliding the small window (bin) from the first to the last in the entire study area. This allows one to get the average for parameters such as the MDA-Chl-*a* (*SST,* SSC) for the entire study area.

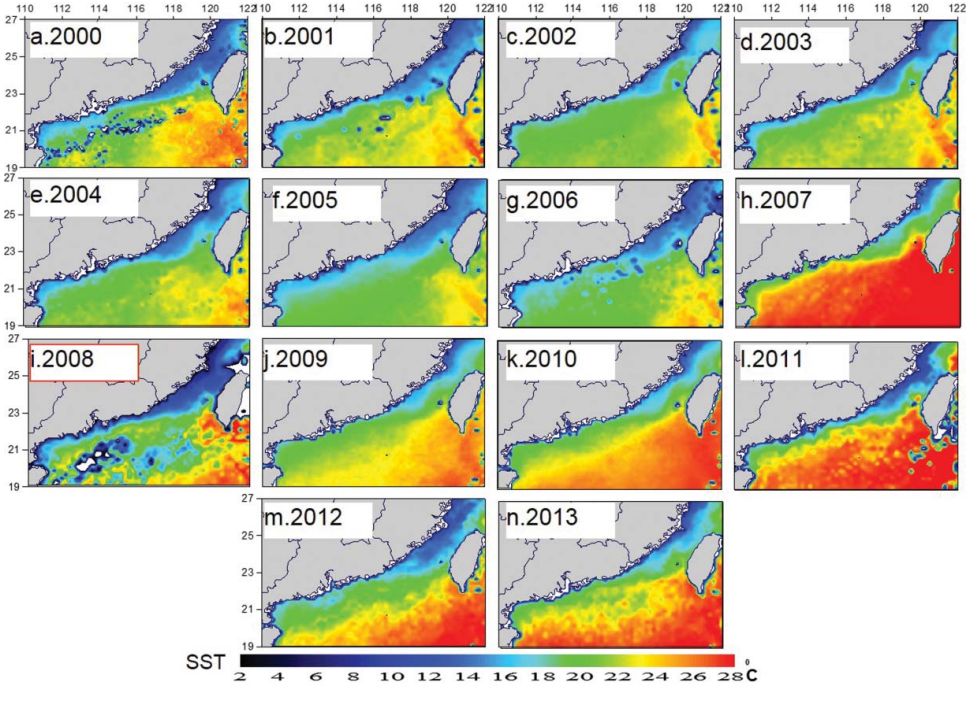

Figure A1. The spatial distribution of SST in the corresponding period (11th January –20th February) from 2000 (a) to 2013(n).

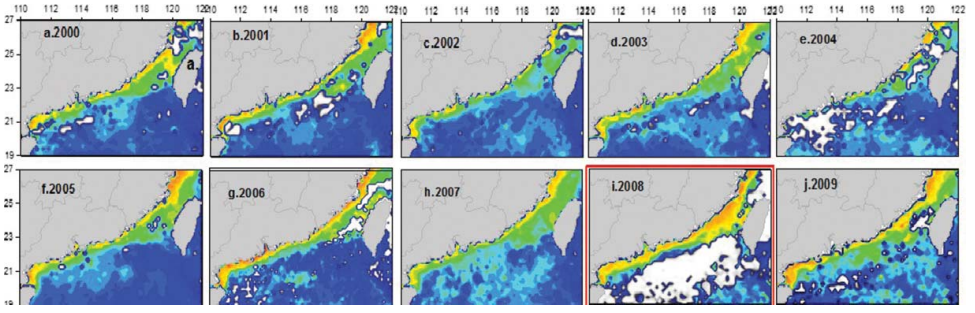

Figure A2. Spatial distribution of Chla concentration from 2000 to 2009. Spatial distribution of MDA-Chla concentration in corresponding time period (from 11th Januaty to 20th February) in the nine years of 2000–2009 in the study area. (a)–(f): 2000–2005, (g)–(i) 2007–2009; Units: mg/m^3.

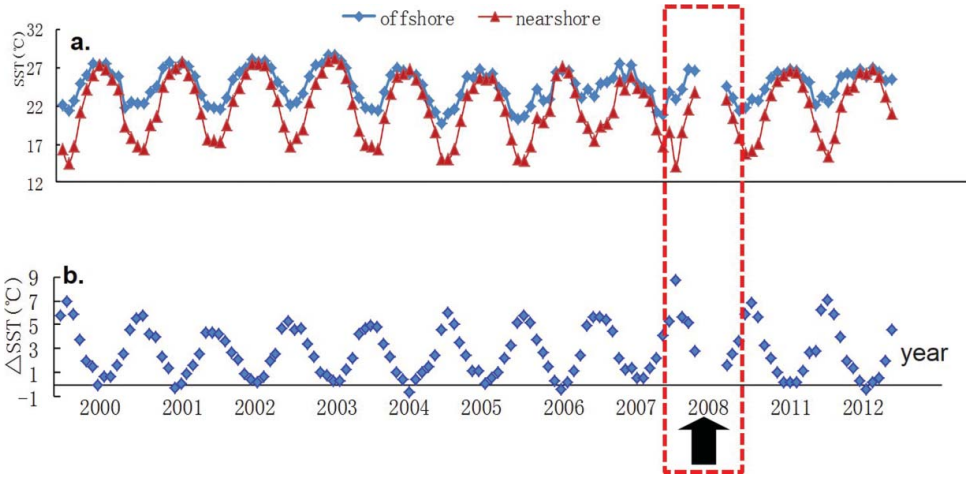

Figure A3. Climatological monthly average SST and its difference in the coastal and offshore waters from 2000 to 2012. (a): Monthly average SST in the coastal and offshore waters; (b): the difference of monthly average SST between offshore and coastal waters.